Applied Physics A (2019) 125:749
https://doi.org/10.1007/s00339-019-3053-3

Applied Physics A
Materials Science & Processing

An extensive investigation of physical, optical and radiation shielding properties for borate glasses modified with gadolinium oxide

Y. Al-Hadeethi[1,2] · M. I. Sayyed[3] · J. Kaewkhao[4] · Bahaaudin M. Raffah[1,2] · Rahma Almalki[1,2] · R. Rajaramakrishna[4]

Received: 23 August 2019 / Accepted: 1 October 2019 / Published online: 9 October 2019

Abstract
We prepared four Gd_2O_3 doped borate glasses and investigated their physical, optical and radiation shielding features. The density of glass samples was increased linearly with the Gd_2O_3 content. The transmission spectra of the samples show more than 85% transmittance suggesting their superior transparency in the visible region. The band gap decreases with increase in Gd_2O_3 content. The Geant4 code was used to find the attenuation factor for the samples between 0.284 and 2.506 MeV. The results demonstrated that the transmission factor changes from 51% (corresponding to 20 mol% of Gd_2O_3) to 39% (for 35 mol%) at 0.284 MeV. The addition of Gd_2O_3 affects highly the mass attenuation parameter at 0.284 and 0.347 MeV. The effective atomic numbers of the glass sample corresponding to 20 mol% of Gd_2O_3 are in the range 12.06–18.79. The maximum tenth value layer was observed for 20 mol% of Gd_2O_3 sample (15.768 cm).

Keywords Borate glasses · Physical properties · Geant4 · Optical band gap · Radiation

1 Introduction

The design and development of appropriate shields is an issue of considerable concern to protect public and workers from continuous exposure to the radiation which is emitted from nuclear research equipment, nuclear reactors and nuclear power plants, in addition to radiation used in different industrial, medical imaging and therapy, archaeological and agricultural applications [1, 2]. At present, glass is vastly utilized as a shielding material against the strongly penetrating radiation like gamma rays due to many reasons such as glass is comparatively low cost, nontoxic, ease of fabrication, transparent to the visible light, and effective shielding attributes [3–8]. Glass samples must have high transparent properties and high density to be used as effective shielding materials against gamma ray. If the density of the glass sample is high, the likelihood of the interaction between the photons and the sample is high and therefore the gamma photons loss their energy quickly and cannot penetrate the sample, so the transmission of the photons through the glass specimen is low. Accordingly, to enhance the attenuation features of any glass, we need to increase the density of this sample [9]. Borate-based glasses have received widespread attention due to their interesting chemical and physical features such as their high chemical durability, low-viscosity, high visible light transparency, low glass transition temperature, good mechanical stability and attainability at low cost [10–12]. Among the characteristics desired for shielding applications, the density is especially important and the incorporation of heavy metal oxides (HMO) and heavy rare-earth oxides (HREO) is one of the simplest methods to increase the density of the glass sample. Gadolinium oxide (Gd_2O_3, density = 7.41 g/cm^3) being one among rare earth ions which provide the platform to co-dope with other rare earths for their efficient energy transfer characteristics incorporated in glasses as activators. Nowadays, glass scintillators with a high concentration of Gd_2O_3 are used in different phosphate, germinate and silicate glass systems with relatively high light yield and speedy decay time [13, 14]. In the literature, numerous works have been achieved to assess the radiation

✉ Y. Al-Hadeethi
yalhadeethi@kau.edu.sa

[1] Department of Physics, Faculty of Science, King Abdulaziz University, Jeddah 21589, Saudi Arabia

[2] Lithog Devices Fabricat and Dev Res Grp, Deanship Sci Res, King Abdulaziz Univ, Jeddah 21589, Saudi Arabia

[3] Department of Physics, Faculty of Science, University of Tabuk, Tabuk, Saudi Arabia

[4] Center of Excellence in Glass Technology and Materials Science (CEGM), Nakhon Pathom Rajabhat University, Nakhon Pathom 73000, Thailand

shielding properties for different materials, but there are a small number of works which investigated the radiation attenuation performance of borate-based glass systems. Wilson [15] used the XCOM program to estimate the gamma ray shielding characteristics of bismuth-borate glasses. The author found that the addition of barium oxide to the samples increases the half value thickness and therefore according to his conclusion, the glass sample which contains 2 mol% of BaO has the best attenuation ability against gamma ray. Sayyed et al. [16] prepared four borate glasses with different amounts of MoO_3 and Bi_2O_3 and reported the structural features of the samples using FTIR and the shielding properties using transmission geometry. The results showed that the addition of Bi_2O_3 from 30 to 45 mol% remarkably improves the ability of the glass to absorb the incoming gamma rays, and the lowest radiation protection efficiency for the samples occurred at 1.33 MeV. Kurudirek [17] investigated the radiation shielding parameters for some heavy metal borate glass samples and compared these parameters with the corresponding parameters with lead glass and some concretes. He found that the bismuth borate glass sample has superior attenuation properties than steel magnetite concrete. Also, he found that the bismuth borate glass has better attenuation properties than lead glass at some energy values. Prabhu et al. [18] prepared zinc bismuth borate glasses with different amounts of Er_2O_3 (between 0.1 and 1 mol%) and studied the effects of irradiating the prepared samples by high gamma photons with energy of 1.3 MeV. Also, the authors calculated some shielding parameters to understand the effects of both, the Er_2O_3 concentration and the energy on the shielding behavior of the prepared samples. The authors concluded that by increasing the concentration of Er_2O_3 as well as the thickness of the glass, more shielding of gamma rays can be attained. Halimah et al. [19] evaluated the impact of Bi_2O_3 on gamma ray shielding features of borotellurite glass. The authors measured the mass attenuation coefficient at 662 keV. Also, they studied the structural properties of the samples after adding different Bi_2O_3 concentrations using FTIR technique. They found that the addition of Bi_2O_3 raises the density value of the sample which enhances the shielding performance of the borotellurite samples. Recently, Kaur et al. [20] fabricated new bismuth borate glass system with different content of BaO and measured the optical properties of the samples using UV–Visible and the structural properties using Raman method. Also, they reported the shielding behavior of the fabricated bismuth borate glasses experimentally at 662 keV and theoretically at different energies. The authors compared the tenth value layer of the fabricated bismuth borate glasses with barite concrete and some other glasses. The G-P fitting approximation helped Singh et al. [21] to estimate the buildup factors of borate heavy metal oxide glasses and also, they utilized the WinXcom to compute the shielding parameters theoretically. The authors discussed the variation of the buildup factors with the glass composition and the energy of the photon. In this work, we prepared four Gd_2O_3 doped borate glasses and investigated their physical, optical and radiation shielding features. The Geant4 code was used to find the attenuation factor for the samples at nine energies varying from 0.284 to 2.506 MeV.

2 Materials and methods

2.1 Experimental

Glass samples were prepared from the composition $x\mathrm{Gd_2O_3}$–$(100-x)\mathrm{B_2O_3}$ (where $x = 20$, 25, 30 and 35 mol%) and chemical of 99.9% Gadolinium Oxide (Gd_2O_3), Boric Acid (H_3BO_3) were used during the preparation process. A pestle and mortar were utilized to grind the chemicals into fine powders then mixed using alumina crucible. Then, melted at 1400 °C by an electrical furnace for 7 h. After complete melting, the molten glasses were quickly poured into a graphite mold and annealed at 500 °C for 3 h before being cooled down to room temperature and then the samples were cut and polished to 1.0 cm × 0.3 cm × 1.5 cm.

2.2 Geant4 simulation

In the characterization of the gamma ray shielding abilities of any material, an experimental set-up consisting of a gamma ray detector, gamma ray source and materials to be studies are needed. In the absence of an experimental set-up, Monte Carlo simulations can be used as a flexible and time saving alternative. Therefore, the entire detector geometry of an HPGe detector produced by Canberra semiconductors has been coded into C++ based Geant4 simulation toolkit [22] which is widely used in the diverse field of physics including detector applications. Along with the HPGe detector, geometry, chemical compositions and the densities of the investigated glasses has been coded into Geant4 to define the glasses into simulations. Gamma ray source and the detector were housed in separate lead shields and a hole with 0.3 cm diameter has been created at the center of both lead shields. The lead shield of gamma source was served to create a narrow photon beam so that Beer-Lamberts' Law used to calculate the mass attenuation coefficients (μ/ρ) of the studied glasses is validated. Lead shield of detector used to minimize the systematical errors and served as collimator. As shown in Fig. 1, glass samples were placed between the source and the detector. Gamma rays with the energies of 0.284 MeV (^{137}Cs), 0.347 MeV (^{60}Co), 0.511 MeV (^{22}Na), 0.662 MeV (^{137}Cs), 0.826 MeV (^{60}Co), 1.173 MeV (^{60}Co), 1.275 MeV (^{22}Na), 1.333 MeV (^{60}Co) and 2.506 MeV (^{60}Co) has been directed onto one surface of the glasses and attenuated photon intensity is detected by the detector.

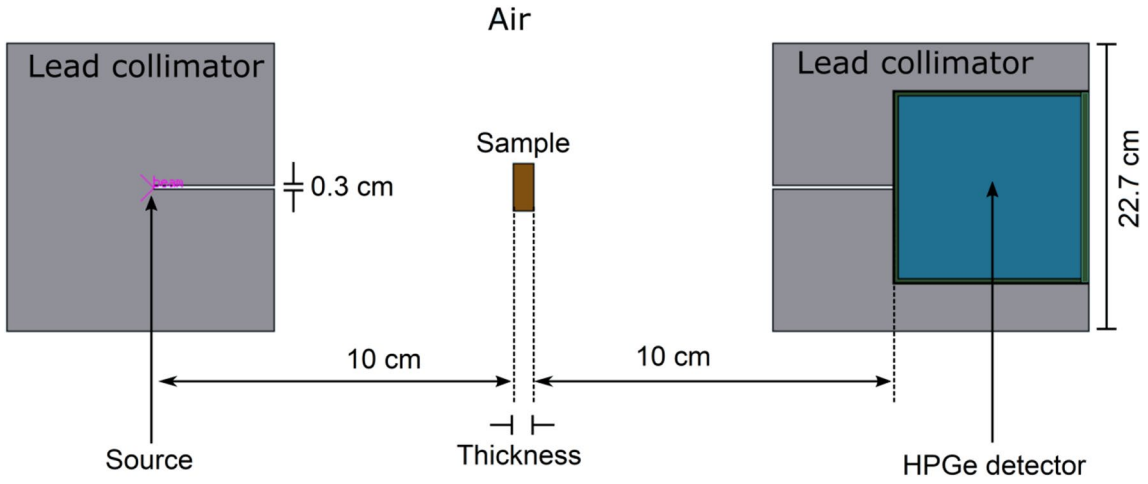

Fig. 1 Schematic of the Geant4 setup used for the determination of the mass attenuation coefficients

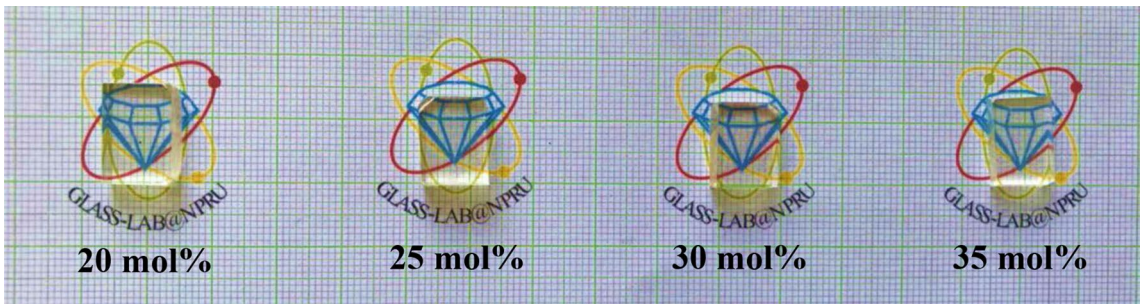

Fig. 2 The glass samples of the Gd_2O_3 doped borate glasses

3 Results and discussion

The synthesized glass samples are illustrated in Fig. 2. From the figure it can be observed that the developed samples show high transparency in all samples. Such clear transparent glasses are very good for shielding properties.

3.1 Optical properties

Figure 3 shows the transmission spectra for the Gd_2O_3–B_2O_3 glasses in the wavelength range 200–2000 nm. The transmission spectra of the glass sample show more than 85% transmittance suggesting their superior transparency in the visible region pointing out their host candidature for optical device applications. Davis and Mott model [23], gives the measure of optical band gap energy which frequently explains the defects observed in density of states or localized states within the mobility gap in amorphous solids. To understand the degree of disorderliness of the absorption coefficient ($\alpha = A/t$), where A is absorbance and t is the thickness of

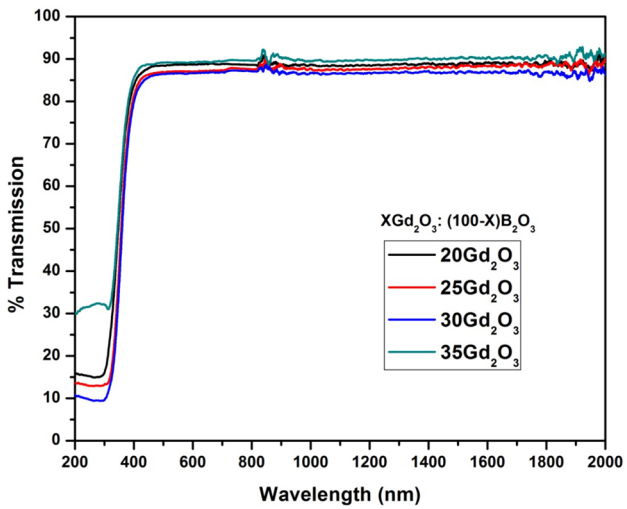

Fig. 3 UV–Vis–NIR transmission spectra of the Gd_2O_3 doped borate glasses

the glass samples. A depends on the incident intensity (I_o) and transmitted (I_t) also referred as $A = \ln(I_o/I_t)$ and related to the photon energy ($h\nu$), optical band gap (E_{opt}) and band

tailing (α_o) through the relation $\alpha(\nu) = \alpha_o\ (h\nu - E_{opt})^n/h\nu$ where $n = 2$ for indirect band gap. Urbach Energy of the samples have been evaluated. In glasses, the exponential law is followed for fundamental absorption edge [23, 30, 31]. Figure 4 shows optical band gap obtained for the fabricated glasses and found to be decreasing with the increase in Gd_2O_3 content as presented in Table 1. The next equation was used to estimate the values of Urbach energy (E) [24, 25].

$$\alpha = \alpha_o \exp\left(\frac{h\nu}{E}\right) \quad (1)$$

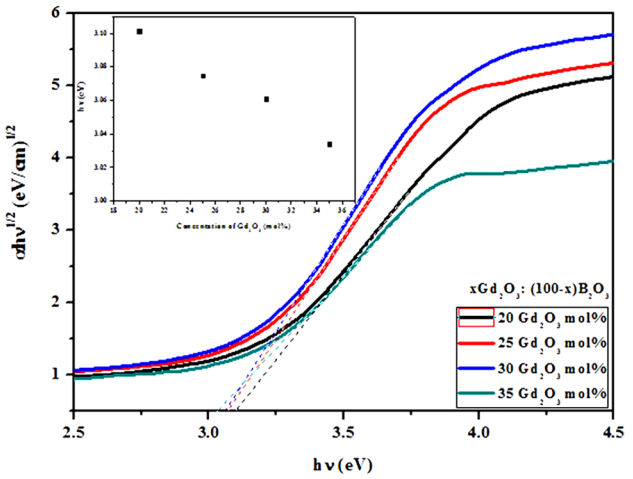

Fig. 4 The optical band gap energy of the Gd_2O_3 doped borate glasses

where α_o is a pre-exponential constant and E indicates the Urbach energy. The values of Urbach energy (E) are derived by taking the reciprocal of the slope of the linear potion in the graph as shown in Fig. 5. The localized or defect states are directly related to the photon energy [26] and random potential variations in the material into the optical band-gap [27], this could be well elaborated such as, the band tail energy determines the valence and conduction bands associated with localized or defect states available in the material which may alter electron transition concerning to these defects. Such electron transition may not occur directly in amorphous materials, but due to their structural defects or disorder, the phonons will assist the electron transition in indirect manner [28, 29]. Following the addition of Gd_2O_3 in the borate glass matrix, it is noticed from Table 1 that the value of Urbach energy (E) is increases up to 30 mol% and then decreases suggesting that the density of localized or defect or disorder states are more within the mobility gap up to 30 mol% and then decreases. In the band structure, the appearance of localized or defect states usually reduces the optical band gap (E_{opt}) as seen and Table 1 [30].

3.2 Physical properties

The present glasses xGd_2O_3–$(100-x)B_2O_3$ (where $x = 20$, 25, 30 and 35 mol%) in general are moisture insensitive and capable of accepting large concentration of rare earth ions without losing their transparency as discussed in above Sect. 3.1. It is worth mentioning that the increase in the

Table 1 Physical properties of the prepared $xGd_2O_3-(100-x)B_2O_3$ glasses

Physical properties	Gd_2O_3 20 mol%	Gd_2O_3 25 mol%	Gd_2O_3 30 mol%	Gd_2O_3 35 mol%
Density (g/cm^3)	3.7235 ± 0.0015	4.0209 ± 0.0016	4.2958 ± 0.0008	4.6028 ± 0.0049
Molar volume (cm^3/mol)	34.429	35.524	36.660	37.396
Refractive index (n)	1.6534	1.6535	1.6535	1.6533
Optical band gap (E_{opt}, eV)	3.101	3.075	3.061	3.034
Urbach energy (E, eV)	0.352	0.450	0.460	0.357
Concentration of Gd^{3+} (×1021 ions/cc)	1.268	1.536	1.786	2.043
Polaron radius (Rp (Å))	3.801	3.566	3.391	3.243
Inter-nuclear Radius (Ri (Å))	9.257	8.684	8.258	7.896
Field strength (F (×10^{21}), cm^{-2})	2.508	2.850	3.151	3.446
Dielectric constant ($\varepsilon = n^2$)	2.733	2.734	2.734	2.733
Molar refraction (R_m, cm^3/mol)	12.609	13.012	13.428	13.694
Cat-ion polarizability (α_{cat}, Å^3)	0.4352	0.5430	0.6508	0.7586
Electronic oxide polarizability (α_O^{2-}, n)	1.5228	1.5402	1.5593	1.5586
Gd to Gd distance (d_{Gd-Gd} (Å))	3.3509	3.4596	3.5773	3.6911
Boron to boron distance (d_{B-B} (Å))	5.3168	4.9878	4.7434	4.5360
Optical basicity (Λ_{th})	0.5733	0.5857	0.5990	0.5985
Molecular polarizability (α_{mol})	5.0038	5.1636	5.3287	5.4344
Oxygen packing density (OPD)	87.135	84.448	81.833	80.221

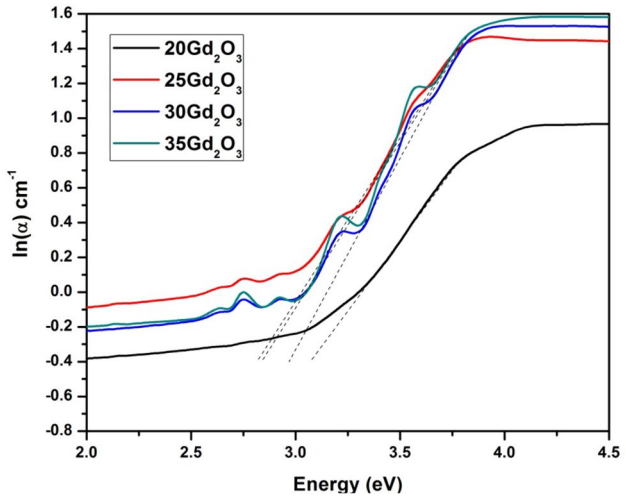

Fig. 5 The dependence of ln(α) of all the compositions on the photon energy ($h\nu$) from which the Urbach energy can be obtained. Solid black dotted lines are best fitted linear fit data

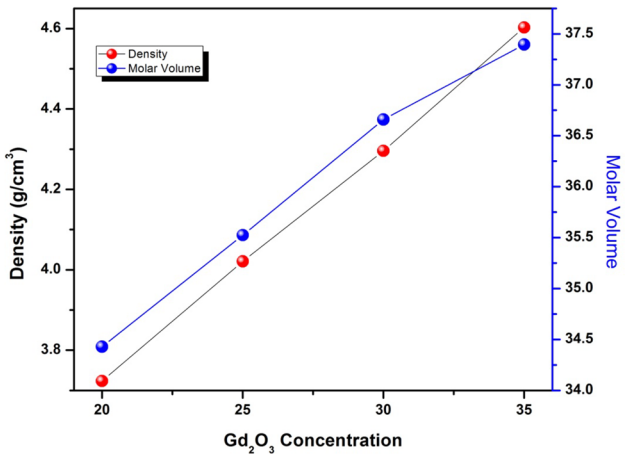

Fig. 6 The density and molar volume of the Gd_2O_3 doped borate glasses

Gd_2O_3 composition in the glass matrix enhances various optical parameters as discussed below.

Figure 6 presents the density and molar volume of glass sample whose results were increased linearly with the Gd_2O_3 content. The molar volume of the glass system increases with the increase in gadolinium content, which is ascribed to the increase in the number of non-bridging oxygen's (NBOs). It may be assumed that the increase in gadolinium content at the expense of B_2O_3 causes the openness in the glass network structure [31, 32]. From Table 1, the refractive index of the glass sample shows almost near values initially then it decreases beyond 30 mol% Gd_2O_3 concentration. In the present case, the glasses show increase in the refractive index value due to the addition of Gd^{3+} ions up to 30 mol%. The refractive index value in general should signify with respect to polarizability. In the present glass the increase in cat-ion polarizability in addition of Gd content decreases the polarizing effect of the cation on to the oxide ion hence refractive index does not show much significance. It should follow general trend with increase in polarizability along with the refractive index, but due to polarizability of the oxide ion depends not only on the refractive index, but also on the molar volume.

At 35 mol% concentration of Gd_2O_3 the non-bridging oxygens (NBOs) convert to bridging oxygens (BOs) hence the refractive index reduces and also slight change in their molar volume occurs as presented in Fig. 6. Concentration of Gd^{3+} ions increases with increase in Gd_2O_3 content, shrinking the borate network hence their inter-nuclear distance and polaron distance reduces. The polaron radius is a vital information to understand their activation energy in the glass matrix which also depends on their oxidation state. In this glass we used Gd^{3+} ions as starting batch component, nature of average Gd^{3+}-Gd^{3+} and Boron–Boron separation which affects their shielding and scintillating property of the glass.

From Table 1 the optical band gap decreases as the average B–B separation $<d_{B-B}>$ and inter-nuclear spacing of Gd^{3+} ion (R_i) values decrease. Such decrease in the values will enhance volume of the matrix and diminishes density of the present glass systems. The RE (rare earth) ions are positioned between the voids and hence average Gd to oxygen distance decreases. As a result of that, the Gd-O bond strength increase, producing a stronger field around the Gd^{3+} ions as observed in the values of field strength from Table 1. The dielectric constant was measured based on refractive index values which increases with the increase in Gd_2O_3 content due to band gap of Gd_2O_3 varies around 3.6–3.7 eV [33] and due to higher molecular weight of Gd_2O_3 compared to that of B_2O_3. The electronic oxide polarizability values increase with increasing Gd_2O_3 content. This is expected as a result of the increase in NBO (non-bridging oxygen's) which is confirmed from their increase in molar volume as discussed above [34]. The optical basicity of the glass increases with increasing Gd_2O_3 content suggesting that the oxygen can bond with their surroundings, hence creating more non bridging oxygen's, while at 35 mol% Gd_2O_3 it restricts to donate their negative charge by making the structure more compactness with their covalency than other concentration. The average total molar polarizability increases with Gd_2O_3 content suggesting that the polarizing species overcomes the network forming species such as boron in the present case and also this is confirmed by their increase in gadolinium to gadolinium separation and decrease in boron to boron separation. In the oxide glasses, the arrangement of oxygen atoms and glass structure is evaluated by oxygen packing density (OPD) using expression reported in [35] and given in Table 1 which shows decreasing trend with the increase in Gd_2O_3 content. Such decreasing trend in OPD

is due to expansion in glass structure and creation of non-bridging oxygen with increase of Gd_2O_3 content.

3.3 Radiation shielding properties

The transmission factor ($TF = I/I_o$) is a term gives a direct indication about the amount of incident photons that are attenuated by the sample. Low TF for a sample indicates more photons are attenuated by the sample. The TF for the Gd_2O_3-B_2O_3 glasses at the investigated energies is presented in Fig. 7. It is clear from the curve that the TF proportionally rises with the energy and falls with the Gd_2O_3 concentration. It is found that the TF changes from 51% (corresponding to 20 mol% of Gd_2O_3) to 39% (for 35 mol% of Gd_2O_3) at 0.284 MeV. While for the same samples at 0.826 MeV, the TF changes from 77 to 71%. For the sample with $30Gd_2O_3$ mol%, the TF at 0.284, 0.347, 0.511, 1.275 and 2.506 MeV are 43, 53, 64, 79 and 84% respectively. This suggests that the TF increases with increasing the energy. On other words, increasing the energy of the photon minimize the attenuation ability of the glass. The maximum amount of TF recorded for the present samples is 87% for the 20 mol% of Gd_2O_3 glass system. It is worth mentioning that the lowest TF occurs at 0.284 MeV for 35 mol% of Gd_2O_3 (which equal to 39%), which means that it can attenuate 61% of the photons at this energy.

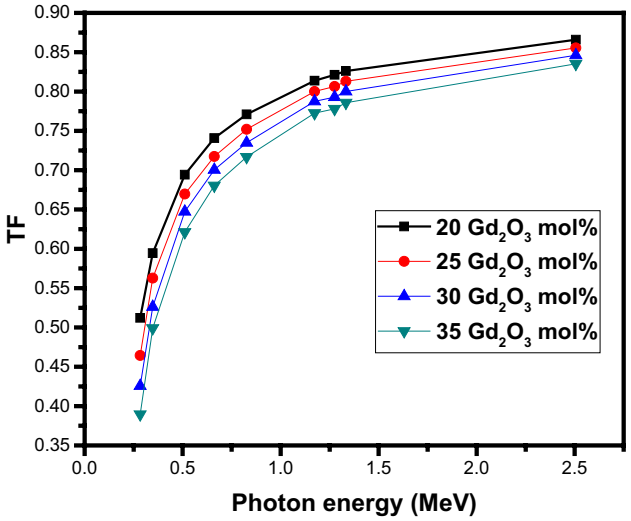

Fig. 7 Variation of the transmission factor with the photon energy for the Gd_2O_3 doped borate glasses

Based on the values of I_0 and I estimated from the Geant4 input file for the present Gd_2O_3–B_2O_3 glasses, the mass attenuation coefficients (μ/ρ) are calculated between 0.284 and 2.506 MeV. The simulated μ/ρ values are compared with WinXcom [36] as shown in Table 2. In comparison of the μ/ρ values simulated by Geant4 to those estimated from WinXcom, it is evident that the μ/ρ values in both methods are close together however there are some acceptable deviations between the two approaches (see Table 2). For example, for 20 mol% of Gd_2O_3 sample, the simulated value of this parameter at 0.284 MeV is 0.1801 cm^2/g, whereas the theoretical value is 0.1857 cm^2/g. The deviation between the Gant4 and WinXcom results for every glass sample range from 0.509 to 3.109%, 0.601 to 3.494%, 0.192 to 2.786% and 0.254 to 3.315% for 20 mol% of Gd_2O_3, 25 mol% of Gd_2O_3, 30 mol% of Gd_2O_3 and 35 mol% of Gd_2O_3 glasses which is considered as small deviation.

In Fig. 8, we plotted the μ/ρ values for the Gd_2O_3–B_2O_3 glasses as a function of Gd_2O_3 at the investigated energies. When μ/ρ of the present samples is examined, considerable increases are observed at 0.284 and 0.347 MeV. For example, the μ/ρ values for both samples 20 mol% of Gd_2O_3 and 35 mol% of Gd_2O_3 at the first energy are 0.1857 and 0.2097 cm^2/g. This implies that the addition of Gd_2O_3 affects highly the attenuation parameter at these energies which is clearly shown in Fig. 8. This behavior in the μ/ρ can be ascribed to higher cross section and density of Gd_2O_3 in comparison with B_2O_3 and the photoelectric effects which is important mechanism at these energies depends highly on the atomic number. From this we can explain the high values of μ/ρ at 0.284 and 0.347 MeV and we can understand why

Table 2 Comparison of mass attenuation coefficients of the B_2O_3–Gd_2O_3 glasses using Geant4 and WinXcom

$35Gd_2O_3$			$30Gd_2O_3$			$25Gd_2O_3$			$20Gd_2O_3$			E (MeV)
Deviation	Geant4	WinXcom	Deviation	Geant4	WinXcom	Deviation	Geant4	WinXcom	Deviation	Geant4	WinXcom	
2.293	0.2050	0.2097	1.957	0.1993	0.2032	2.251	0.1910	0.1953	3.109	0.1801	0.1857	0.284
3.173	0.1513	0.1561	1.939	0.1496	0.1525	3.494	0.1431	0.1481	2.074	0.1398	0.1427	0.347
1.834	0.1036	0.1017	0.887	0.1015	0.1006	0.601	0.0999	0.0993	0.509	0.0982	0.0977	0.511
2.265	0.0839	0.0820	2.043	0.0832	0.0815	1.816	0.0826	0.0811	0.495	0.0808	0.0804	0.662
3.315	0.0724	0.0700	2.786	0.0718	0.0698	1.831	0.0710	0.0697	0.572	0.0699	0.0695	0.826
0.710	0.0563	0.0559	0.179	0.0559	0.0560	0.718	0.0557	0.0561	1.261	0.0555	0.0562	1.173
2.564	0.0546	0.0532	1.479	0.0541	0.0533	0.000	0.0535	0.0535	1.130	0.0531	0.0537	1.275
1.143	0.0525	0.0519	0.192	0.0520	0.0521	1.163	0.0516	0.0522	1.946	0.0514	0.0524	1.333
0.254	0.0393	0.0394	0.510	0.0392	0.0394	0.769	0.0390	0.0393	0.771	0.0389	0.0392	2.506

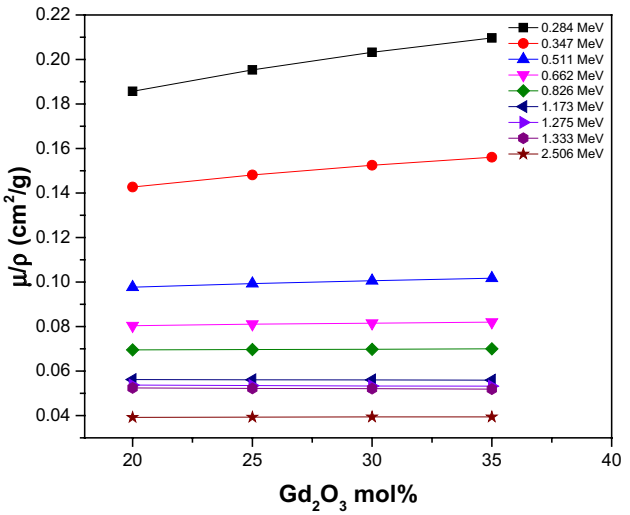

Fig. 8 Variation of the mass attenuation coefficient with Gd_2O_3 content at photon energies 0.284–2.506 MeV

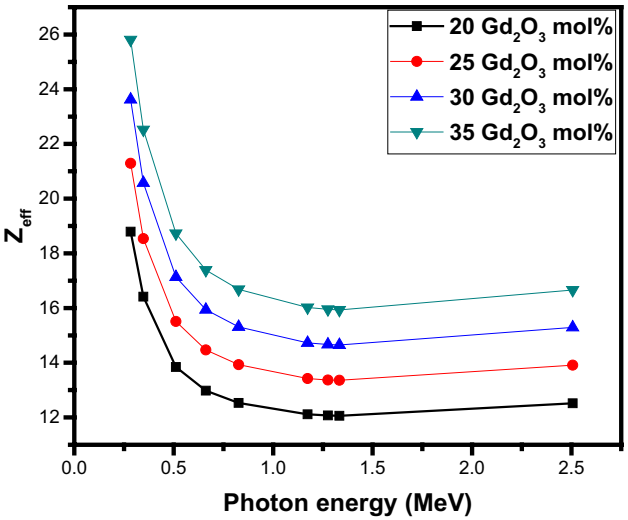

Fig. 9 Variation of the effective atomic number (Z_{eff}) with the photon energy for the Gd_2O_3 doped borate glasses

35 mol% of Gd_2O_3 sample (contains the maximum weight fraction of the high atomic number element namely Gd, $Z=64$) has the highest values at 0.284 MeV. This result indicates that the interaction of the gamma photons with the investigated glasses is high at lower energies, therefore the attenuation of the glasses is relatively high at low energy, while as the energy increases, the reduction in μ/ρ values mean that the transmission of gamma photons through the B_2O_3–Gd_2O_3 glasses is high and thus photons can penetrate the samples easily. Furthermore, from Fig. 8 no considerable difference in the attenuation parameter can be noticed for 0.826 MeV $< E \leq$ 2.506 MeV which is attributed to the domination of Compton scattering. For instance, the μ/ρ for the B_2O_3–Gd_2O_3 glasses with 20 and 35 mol% of Gd_2O_3 are 0.0392 and 0.0394 cm^2/g at 2.506 MeV. For the same samples and at 1.275 MeV, the values are 0.0537 and 0.0532 cm^2/g.

The probability of the interaction of energetic photons with the Gd_2O_3–B_2O_3 glasses can be studied in terms of another factor known as the effective atomic number (Z_{eff}), which can be obtained mathematically according to the following equation:

$$Z_{\text{eff}} = \frac{\sum_i f_i A_i \left(\frac{\mu}{\rho}\right)_i}{\sum_i f_i \frac{A_i}{} \left(\frac{\mu}{\rho}\right)_i} \tag{2}$$

We presented the Z_{eff} for the borate glasses with different Gd_2O_3 concentration (varying from 20 to 35 mol%) in Fig. 9. In general, any glass sample contains HMO (like Gd_2O_3) has a comparatively high Z_{eff}. Referring to Fig. 9, it is evident that the Z_{eff} of the samples increasing with the addition of Gd_2O_3. This is attributed to the high atomic number of Gd ($Z=64$) compared to B ($Z=5$). Increasing the content of Gd in the structure of the glasses will increase the gamma ray-Gd atoms interaction and this which in turn decreases the transmitted gamma ray via the glass specimen. From this result we can say that the 35 mol% Gd_2O_3 doped borate glass sample is the superior attenuator sample. The Z_{eff} values of the glass sample corresponding to 20 and 35 mol% of Gd_2O_3 are in the range of 12.06–18.79 and 15.93–25.81, respectively. On the other hand, Z_{eff} shows a decreasing order as the energy changes from 0.284 to 1.33 MeV and a very slight increasing in the Z_{eff} value observed at the higher energy (i.e. 2.506 MeV). This increase at higher energy maybe ascribed to the pair production which start dominating at $E > 1.02$ MeV [21]. For the Gd_2O_3 doped borate glasses, we calculated the sample thickness which attenuates the photons to one-tenth of the original value. This is known as the tenth value layer (TVL) and depends basically on the density of the medium. The following relation helped to find the TVL for the Gd_2O_3–B_2O_3 glasses:

$$\text{TVL} = \frac{\text{In}^{10}}{\mu} \tag{3}$$

The TVL dependency of the investigated Gd_2O_3-borate glasses on the energy is exhibited in Fig. 10. Apparently, the TVL fall with increasing the concentration of Gd_2O_3 from 20 to 35 mol% which is ascribed to the increase in the density as shown in Table 1, and the TVL rises with increasing the energy from 0.284 to 2.506 MeV. The TVL dependency on the energy and Gd_2O_3 content demonstrated that more gamma ray intensity being shielding

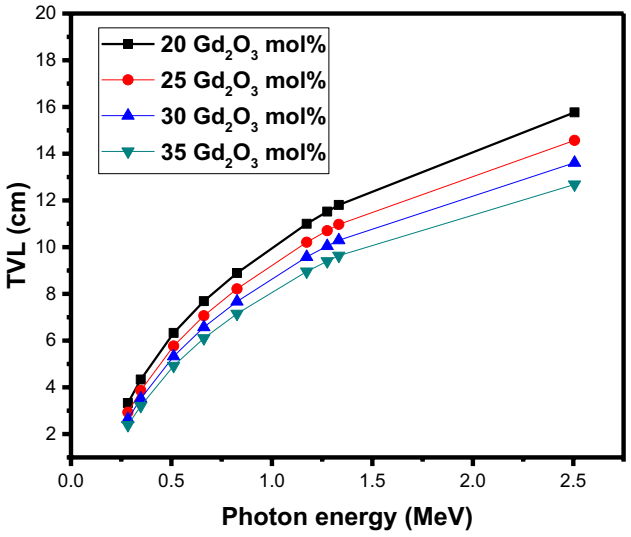

Fig. 10 Variation of the tenth value layer (cm) with the photon energy for the Gd_2O_3 doped borate glasses

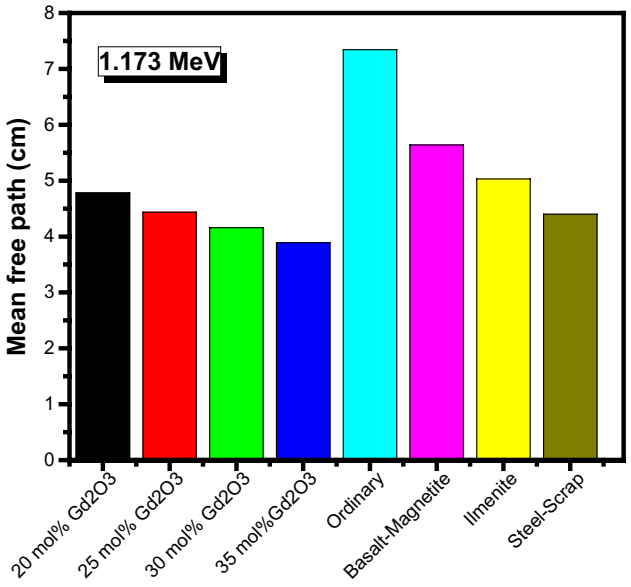

Fig. 11 Comparison of the mean free path of the investigated glasses with some concretes at 1.173 MeV

in the higher Gd_2O_3 content and low photon energy. The maximum TVL value observed for 20 mol% of Gd_2O_3 sample (15.768 cm) and this means that 15.768 cm thickness of this sample is needed to absorb 90% of the intensity of gamma ray. While, the minimum TVL is found for 35 mol% of Gd_2O_3 sample at 0.284 MeV and equal to 2.386 cm. The TVL curve shows that the addition of Gd_2O_3 improves the shielding efficiency of the current Gd_2O_3 doped borate glasses. In Fig. 11, we compared the mean free path (MFP) for Gd_2O_3 doped borate glasses

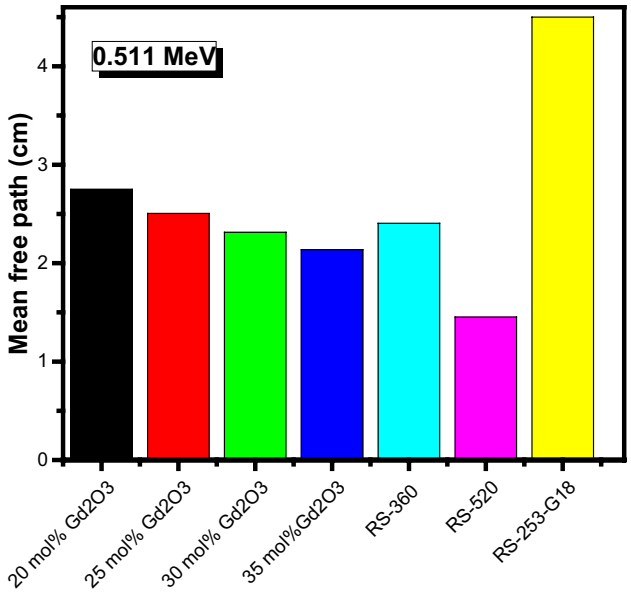

Fig. 12 Comparison of the mean free path of the investigated glasses with some commercial glasses at 0.511 MeV

with some concretes [37] widely used for the shielding aims at 1.173 MeV, while in Fig. 12 we compared the MFP for the Gd_2O_3 doped borate glasses with commercial glasses [38]. The MFP is an important attenuating factor and represents the distance that a radiation can move in a sample without having any type of scattering or absorbing. Practically, low MFP for the sample implies the good attenuating performance of this sample. It is clear that all the fabricated Gd_2O_3 doped borate glasses have lower MFP than ordinary, ilmenite and basalt-magnetite concretes at 1.173 MeV, while steel-scrap concrete has almost the same MFP with 25 mol% Gd_2O_3 sample. From Fig. 12, all the present glasses have lower MFP than RS-253-G18 and higher MFP than RS-520, whereas 25 mol% Gd_2O_3 sample has almost the same MFP with RS-360.

4 Conclusion

We successfully prepared four Gd_2O_3 doped borate glasses and reported their physical, optical and gamma rays shielding characteristics. The transmission spectra of the glass sample show more than 85% transmittance suggesting their superior transparency in visible region suggesting their host candidature for optical device applications. The density of the samples increases from 3.7235 to 4.6028 g/cm^3 while the optical band gap decreases from 3.101 to 3.034 as the Gd_2O_3 content increases from 20 to 35 mol%. The Geant4 code was used to investigate the TF and μ/ρ for the current samples and the results showed that the maximum amount of TF recorded for the present samples is 87% for the 20 mol% of Gd_2O_3 glass, and the lowest TF occurs at 0.284 MeV for

35 mol% of Gd_2O_3 (which equal to 39%). The TVL falls with increasing the concentration of Gd_2O_3 from 20 to 35 mol%, and rises with increasing the energy from 0.284 to 2.506 MeV. The maximum TVL values observed for 20 mol% of Gd_2O_3 sample (15.768 cm). Besides, we compared the MFP for Gd_2O_3 doped borate glasses with some concretes and with commercial glasses. All the prepared Gd_2O_3 doped borate samples possess lower MFP than ordinary, ilmenite and basalt-magnetite concretes at 1.173 MeV, while steel-scrap concrete has almost the same MFP with 25 mol% Gd_2O_3 sample.

Acknowledgements This project was funded by the Deanship of Scientific Research (DSR), King Abdulaziz University, Jeddah, under Grant No. (KEP-Msc-6-130-40). The authors, therefore, gratefully acknowledge the DSR technical and financial support.

References

1. B. Pomaro, F. Gramegna, R. Cherubini, V. De Nadal, V. Salomoni, F. Faleschini, Gamma-ray shielding properties of heavyweight concrete with Electric Arc Furnace slag as aggregate: an experimental and numerical study. Constr. Build. Mater. **200**, 188–197 (2019)
2. P. Lotti, D. Comboni, L. Gigli, L. Carlucci, E. Mossini, E. Macerata, G. Mario Mariani, D. Gatta, Thermal stability and high-temperature behavior of the natural borate colemanite: an aggregate in radiation-shielding concretes. Constr. Build. Mater. **203**, 679–686 (2019)
3. M.I. Sayyed, H.O. Tekin, E.E. Altunsoy, S.S. Obaid, M. Almatari, Radiation shielding study of tellurite tungsten glasses with different antimony oxide as transparent shielding materials using MCNPX code. J. Non-Cryst. Solids **498**, 167–172 (2018)
4. M.I. Sayyed, G. Lakshminarayana, M.G. Dong, M. Çelikbilek Ersundu, A.E. Ersundu, I.V. Kityk, Investigation on gamma and neutron radiation shielding parameters for $BaO/SrO-Bi_2O_3-B_2O_3$ glasses. Radiat. Phys. Chem. **145**, 26–33 (2018)
5. A. Kumar, M.I. Sayyed, M. Dong, X. Xue, Effect of PbO on the shielding behavior of $ZnO–P_2O_5$ glass system using Monte Carlo simulation. J. Non-Cryst. Solids **481**, 604–607 (2018)
6. M.I. Sayyed, G. Lakshminarayana, Structural, thermal, optical features and shielding parameters investigations of optical glasses for gamma radiation shielding and defense applications. J. Non-Cryst. Solids **487**, 53–59 (2018)
7. O. Agar, M.I. Sayyed, H.O. Tekin, K.M. Kaky, S.O. Baki, I. Kityk, An investigation on shielding properties of BaO, MoO_3 and P_2O_5 based glasses using MCNPX code. Results Phys. **12**, 629–634 (2019)
8. G. Lakshminarayana, A. Kumar, M.G. Dong, M.I. Sayyed, N.V. Long, M.A. Mahdi, Exploration of gamma radiation shielding features for titanate bismuth borotellurite glasses using relevant software program and Monte Carlo simulation code. J. Non-Cryst. Solids **481**, 65–73 (2018)
9. O. Agar, Z.Y. Khattari, M.I. Sayyed, H.O. Tekin, S. Al-Omari, M. Maghrabi, M.H.M. Zaid, I.V. Kityk, Evaluation of the shielding parameters of alkaline earth based phosphate glasses using MCNPX code. Results Phys. **12**, 101–106 (2019)
10. S.B. Kolavekar, N.H. Ayachit, G. Jagannath, N. Krishnakanth, S. Venugopal Rao, Optical, structural and Near-IR NLO properties of gold nanoparticles doped sodium zinc borate glasses. Opt. Mater. **83**, 34–42 (2018)
11. E.C. Paz, J.D.M. Dias, G.H.A. Melo, T.A. Lodi, J.O. Carvalho, P.F. Façanha Filho, M.J. Barboza, F. Pedrochi, A. Steimacher, Physical, thermal and structural properties of Calcium Borotellurite glass system. Mater. Chem. Phys. **178**, 133–138 (2016)
12. M. Mariyappan, K. Marimuthu, M.I. Sayyed, M.G. Dong, U. Kara, Effect Bi_2O_3 on the physical, structural and radiation shielding properties of Er^{3+} ions doped bismuth sodiumfluoroborate glasses, J. Non-Cryst. Solids 499 (2018) 75–85
13. H. Luo, H. Xiaolin, W. Liu, Y. Zhang, L. Anxian, X. Hao, Compositional dependence of properties of $Gd_2O_3–SiO_2–B_2O_3$ glasses with high Gd2O3 concentration. J. Non-Cryst. Solids **389**, 86–92 (2014)
14. X.-Y. Sun, D.-G. Jiang, W.-F. Wang, C.-Y. Cao, Y.-N. Li, G.-T. Zhen, H. Wang, X.-X. Yang, H.-H. Chen, Z.-J. Zhang, J.-T. Zhao, Luminescence properties of B2O3–GeO2–Gd2O3 scintillating glass doped with rare-earth and transition-metal ions. Nucl. Instrum. Methods Phys. Res. A **716**, 90–95 (2013)
15. M. Wilson, Optimization of the radiation shielding capabilities of bismuth-borate glasses using the genetic algorithm. Mater. Chem. Phys. **224**, 238–245 (2019)
16. M.I. Sayyed, Kawa M. Kaky, D.K. Gaikwad, O. Agar, U.P. Gawai, S.O. Baki, Physical, structural, optical and gamma radiation shielding properties of borate glasses containing heavy metals (Bi_2O_3/MoO_3), J. Non-Cryst. Solids **507,** 30–37 (2019)
17. M. Kurudirek, Heavy metal borate glasses: potential use for radiation shielding. J. Alloy. Compd. **727**, 1227–1236 (2017)
18. Nimitha S. Prabhu, Vinod Hegde, M.I. Sayyed, O. Agar, Sudha D. Kamath, Investigations on structural and radiation shielding properties of Er^{3+} doped zinc bismuth borate glasses. Mater. Chem. Phys. **230** (2019) 267–276
19. M.K. Halimah, A. Azuraida, M. Ishak, L. Hasnimulyati, Influence of bismuth oxide on gamma radiation shielding properties of borotellurite glass. J. Non-Cryst. Solids **512**, 140–147 (2019)
20. Parminder Kaur, K.J. Singh, Sonika Thakur, Prabhjot Singh, B.S. Bajwa, Investigation of bismuth borate glass system modified with barium for structural and gamma-ray shielding properties, Spectrochimica Acta Part A: Mol. Biomol. Spectrosc. **206** (2019) 367–377
21. V.P. Singh, N.M. Badiger, J. Kaewkhao, Radiation shielding competence of silicate and borate heavy metal oxide glasses: comparative study. J. Non-Cryst. Solids **404**, 167–173 (2014)
22. S. Agostinelli, J. Allison, K. Amako, J. Apostolakis, H. Araujo et al., Geant4-a simulation toolkit. Nucl. Instr. Meth. Phys. A **506**, 250–303 (2003)
23. E.A. Davis, N.F. Mott, Conduction in non-crystalline systems V. Conductivity, optical absorption and photoconductivity in amorphous semiconductors. Philos. Mag. **22**, 903–922 (1970)
24. F. Urbach, The long-wavelength edge of photographic sensitivity and of the electronic absorption of solids. Phys. Rev. **92**, 1324 (1953)
25. A.S. Hassanien, A.A. Akl, Effect of Se addition on optical and electrical properties of chalcogenide CdSSe thin films. Superlattice. Microst. **89**, 153–169 (2016)
26. M. Zanini, J. Tauc, temperature dependence of the absorption edge of liquid sulfur. J. Non-Cryst. Solids **23**, 349 (1977)
27. A.A. Kutub, A.E. Mohamed-Osman, C.A. Hogarth, Some studies of the optical properties of copper phosphate glasses containing praseodymium. J. Mater. Sci. **21**, 3517 (1986)
28. C. Dayanand, G. Bhikshamaiah, M. Salagram, IR and optical properties of PbO glass containing a small amount of silica. Mater. Lett. **23**, 309 (1995)
29. K.L. Chopra, S.K. Bahl, Exponential tail of the optical absorption edge of amorphous semiconductors. Thin Solid Films **11**, 377 (1972)

30. N.F. Mott, E.A. Davis, *Electronic Processes in Non-crystalline Materials* (Clarendon Press, Oxford, 1979), pp. 3–215
31. I. Khan, G. Rooh, R. Rajaramakrishna, N. Srisittipokakun, C. Wongdeeying, N. Kiwsakunkran, N. Wantana, H.J. Kim, J. Kaewkhao, S. Tuscharoen, J. Alloy. Compd. **774**, 244–254 (2019)
32. S. Kaewjaeng, S. Kothan, W. Chaiphaksa, N. Chanthima, R. Rajaramakrishna, H.J. Kim, J. Kaewkhao, Radiat. Phys. Chem. **160**, 41–47 (2019)
33. S. Horoz, S. Simsek, S. Palaz, A.M. Mamedov, World J. Cond. Matter Phys. **5**, 78–85 (2015)
34. P. Chimalawong, J. Kaewkho, C. Kedkaew, P. Limsuwan, J. Phys. Chem. Solids **71**, 965–970 (2010)
35. M.A. Algradee, M. Sultan, O.M. Samir, A. Elwhab, B. Alwany, Appl. Phys. A **123**, 524 (2017)
36. L. Gerward, N. Guilbert, K.B. Jensen, H. Levring, WinXCom—a program for calculating X-ray attenuation coefficients. Radiat. Phys. Chem. **71**, 653–654 (2004)
37. I.I. Bashter, calculation of radiation attenuation Coefficients for shielding concretes. Ann. Nucl. Energy **24**(17), 1389–1401 (1997)
38. P. Kaur, K.J. Singh, S. Thakur, P. Singh, B.S. Bajwa, Investigation of bismuth borate glass system modified with barium for structural and gamma-ray shielding properties. Spectrochim. Acta Part A Mol. Biomol. Spectrosc. **206**, 367–377 (2019)